23rd ABCM International Congress of Mechanical Engineering
December 6-11, 2015, Rio de Janeiro, RJ, Brazil

MICROSTRUCTURAL ANALYSIS THROUGH TRIDIMENSIONAL INVERSE HEAT TRANSFER MODEL IN GTA ALUMINUM ALLOY WELDING

Elisan dos Santos Magalhães
Edmilson Otoni Corrêa
Ana Lúcia Fernandes de Lima e Silva
Sandro Metrevelle Marcondes Lima e Silva
Heat Transfer Laboratory – LabTC, Institute of Mechanical Engineering – IEM, Federal University of Itajubá – UNIFEI, Campus Prof. José Rodrigues Seabra, Av. BPS, 1303, 37500-903, Itajubá, MG, Brazil.
elisanmagalhaes@hotmail.com, ecotoni@unifei.edu.br, alfsilva@unifei.edu.br, metrevel@unifei.edu.br.

Abstract. *In order to study the Heat Affected Zone (HAZ) in GTA aluminum 6060 T5 alloy welding, a previously developed numerical software based on the tridimensional diffusion equation with moving source and phase change was used. The amount of heat flux delivered to the plate was minimized through a non-linear interactive BFGS (Broydon-Fletcher-Goldfarb-Shanno) inverse technique. GTA welding experiments were performed using thin aluminum plates in four t+ experimental conditions. These plates were cut on the HAZ and were analyzed using an optical microscope. Through the peak temperatures and heating rate obtained by the software, the grain size throughout the HAZ during age hardening was studied. The study found a linear correlation between the grain size on the HAZ and the positive polarity. The study also presented that the cooling rate after the GTAW torch is off is the same for the fusion zone, HAZ and base material. Consequently, the significant change on the microstructure occurs while the GTAW torch is turned on.*

Keywords: *inverse problems, heat flux, temperature estimation, GTAW process, microstructural analysis.*

1. INTRODUCTION

Although several new processes to join metals have been developed, the fusion welding still plays a major role in engineering progress. Hence, a deep understanding of the behavior of microstructural welding is extremely important to minimize potential failures. A fundamental pattern that changes the microstructure is the HAZ (Heated Affected Zone). This factor is the result of the thermal cycle that conducts the recrystallization in welding (Goldak and Akhlaghi, 2005). The thermal cycle is composed basically of two steps, heating and cooling. Although the heating rate is important to achieve the fusion, the cooling rate is extremely important for welding quality. Thus, several studies have been taken into account about the microstructural dependence on cooling rate (Casalino and Panella, 2007; Vishwakarma *et al*., 2008; Amirthalingam *et al*., 2009; Ghosh *et al*., 2010).

The cooling rate could be obtained through a numerical thermal model. Several researchers are using numerical thermal models for the prediction of microstructure parameters (Grill, 1981; Dagner *et al*., 2008; Unfried *et al*., 2009). However, major simplifications are constantly being made to reduce the complexity of this kind of model. This is the case of Unfried *et al*. (2008). In their work, they assumed a one-dimensional heat flux and a one-dimensional thermal model based on the Rosenthal's model. In fact, due to some experimental singularities, as the non-uniformity of the torch arc and the electrical interference on measurements in aluminum welding, a three-dimensional numerical thermal model that covers all boundary conditions is highly complex. In addition, measuring directly the heat flux during process is expensive. However, the use of inverse problems allows a quick determination of this parameter (Carvalho *et al*., 2006). Lately, several studies have been using inverse models to estimate the amount of heat flux delivered on diverse processing (Gonçalves *et al*., 2010; Chen and Yang, 2010; Karkhin *et al*., 2011; Yu-Ching *et al*., 2011; Gostimirovic *et al*, 2011).

A common process extensively used to weld aluminum alloys is the GTAW (Gas Tungsten Arc Welding). Lately, several authors have been conducting studies on microstructure analysis in this welding process. Kumar *et al*. (2007) presented a mathematical model to predict the grain size in the fusion zone on an AA6061 GTAW process. In this work, the authors correlated the peak current and the pulse frequency as inversely proportional to the grain diameter. Manti *et al*. (2008) studied the microstructure and hardness of an AA6061 alloy considering the variation of some pulsed GTAW parameters as pulse duration, peak current and pulse frequency. In their work, the authors found a finer grain structure on the pulsed GTAW process than a conventional TIG welding. Similar studies are continually being performed, (Norman *et al*., 1999; Ahmad *et al*., 2007; Hajbagheri *et al*., 2008).

In the this work, a previously validated homemade C++ code (Magalhães *et al*., 2015) based on the non-linear three-dimensional heat diffusion equation with phase change and moving heat source is applied to determine the cooling rate in the HAZ on a welded plate of AA6060-T5. The samples were cut on the welded region and analyzed through an electronic microscope. The heating and cooling rates were compared with the microstructures found and grain size of the HAZ.

2. MATERIAL, EXPERIMENTS AND SIMULATIONS

The 6060-T5 250mm long, 38mm wide and 6.5mm thick aluminum plates (Mn 0.15%; Fe 0.20%; Mg 0.45%; Si 0.40%; Cu 0.02%; Zn 0.05%; Ti 0.01%) have been welded through a GTA process at LAPROSOLDA (Federal University of Uberlândia – Brazil). The experimental temperatures were collected on accessible points of the sample. An automated system was used with the weld velocity of 250 mm/min. Four *t*+ experimental conditions, 2ms, 7ms, 11ms and 13ms were performed on each of the four experiments in order to assure the repeatability of the results. After the weld, the samples were cut on the weld region and prepared for metallographic specimens. Those preparations and analysis were conducted at the Materials Laboratory of the Federal University of Itajubá (UNIFEI). A concentrated solution of Keller's etch was prepared to visualize the microstructure (Mohammadtaheri, 2012).

In order to simulate the problem, the software took a non-uniform mesh with 225.000 volumes into account. The software collected temperatures values from 6 different points as shown in Fig. 1. Points P_1 and P_2 are positioned in the fusion zone, P_3 and P_4 in the HAZ, finally, P_5 and P_6 in the Base Material.

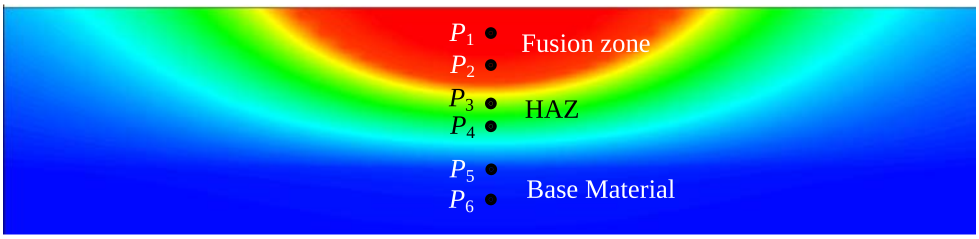

Figure 1. Collected temperature points.

The heating rate was defined as the positive numerical derivative of the collected points and can be expressed as:

$$\frac{\partial T(x,y,z,t)}{\partial t} = \frac{T_{P_i}^{a+1} - T_{P_i}^{a}}{\Delta t}, \tag{1}$$

where T is the temperature, x, y and z the Cartesian coordinates of the respective points P_i, i is the point index and a is the time step.

3. RESULTS ANALYSIS

For each *t*+ condition, the temperature field was determined through the C++ homemade code. The heating rate in the fusion zone could be calculated by the software. Figure 2 presents the temperature fields in the analyzed section for the experimental condition *t*+ = 11ms at instant 6.6s.

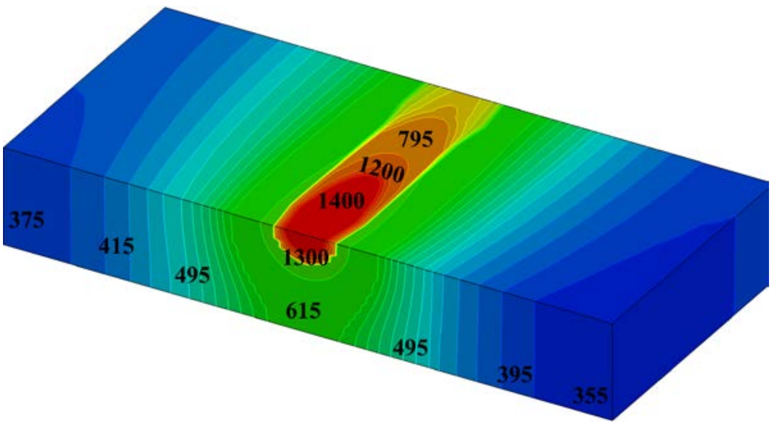

Figure 2. Temperature [°C] distribution for *t*+ = 11ms, at instant 6.6s.

Figure 2 also shows that the highest temperatures on the plate are achieved on the surface close to the GTA arch. In order to validate the program, the width and penetration of the weld bead were collected on the plates and numerically calculated. Table 1 presents the average of the obtained data of these parameters for the four positive polarities on the plate tested. It is worth mentioning that the numerical results present a low deviation from the experimental analysis, which could be considered as a good approach due to the fact that they represent an error of less than 4%.

Table 1. Width and penetration of the weld bead compared numerically and experimentally

Adjusted (*t*+) (ms)	**Experimental Penetration (mm)**	**Numerical Penetration (mm)**	**Experimental Width (mm)**	**Numerical Width (mm)**
2	1.43	1.38	6.22	6.12
7	1.61	1.58	6.66	6.59
11	1.72	1.70	6.76	6.70
13	1.73	1.71	6.77	6.74

As previously mentioned, six numerical sensors were coupled on the software. The heating rate calculated from the numerical temperatures is much more precise than the constant values adopted from handbooks. As a matter of fact, it considers the temperature function and the Cartesian coordinate on the sample. Figure 3 and 4 present the heating rate for the four positive polarities on the sample tested. In all presented cases, point P_1 is subject to the highest temperature gradient. Indeed, this point is nearer to the surface and has the highest influence of the torch arch than the other points. Although point P_2 is also in the fusion zone, it has a lower heating rate when compared with $P1$. Naturally, the temperature in P_2 tends to receive a lower influence of the voltaic arch whereas the heat flux is distributed in the fusion zone. The points in the HAZ, $P3$ and $P4$, have a lower heating rate in relation to P_1 and P_2. From the graphics analysis, the cooling rate of these points, i.e. the negative heating rate presented in Fig. 3 and 4, are more constant than the cooling rate of points P_1 and P_2. Since these points are in the HAZ, the heat delivered by the torch arch is not sufficient to achieve the melting point. However, these points are heated enough to achieve the recrystallization point, which means that they have a bigger grain size when compared to the base metal. The points P_5 and P_6 are in the base metal part of the sample. Consequently, they are not affected by the temperature gradient on the sample. From the heating rate analysis (Figs. 3 and 4) these points are heated in the beginning of the process. However, they do not have a significant cooling rate after time 4s. These points do not achieve the melting point or the recrystallization temperature. As the torch keeps its movement, these points tend to stabilize their temperatures. Consequently, after the torch is off, they have a stable cooling rate which will lead to the same structure of the base material.

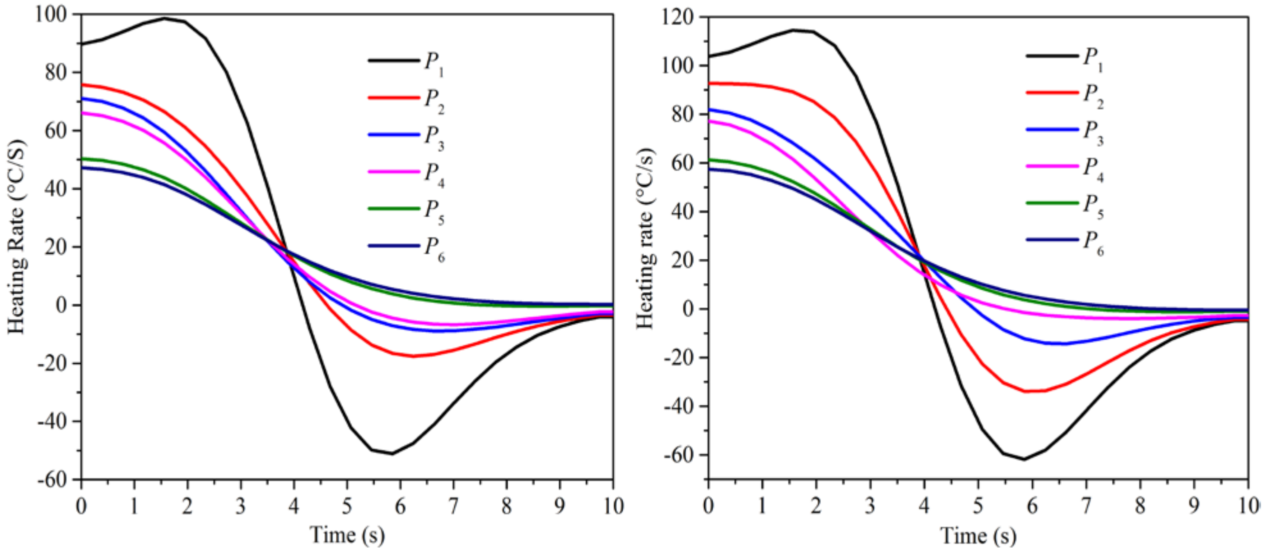

a) b)

Figure 3. Numerical heating rate for *t*+ experimental conditions a) 2ms and b) 7ms

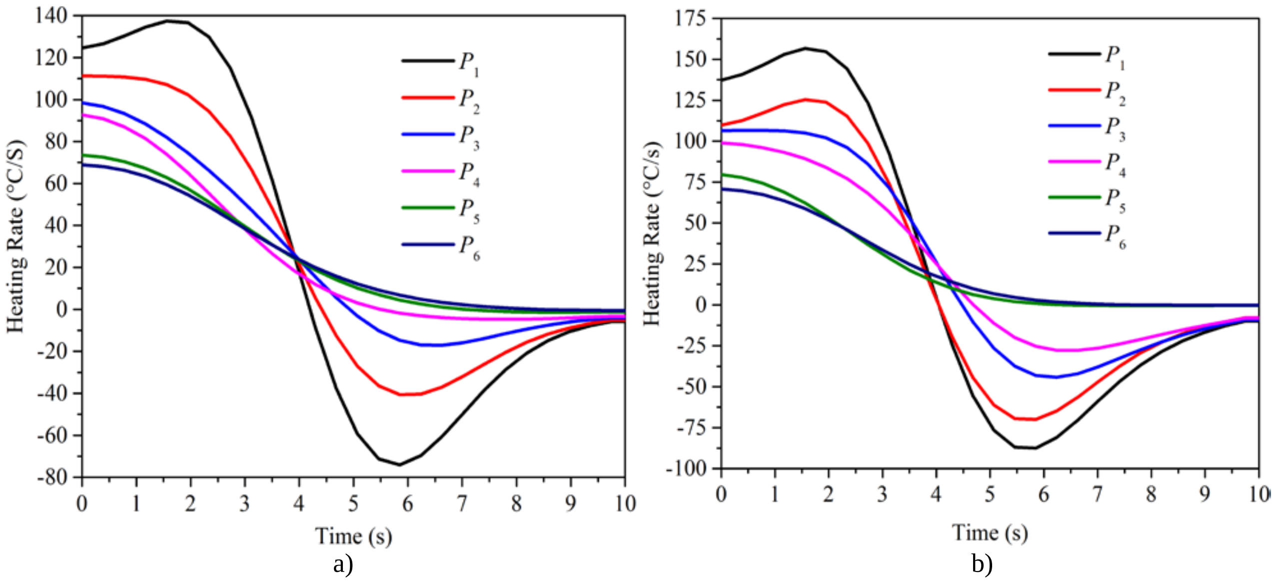

Figure 4. Numerical heating rate for *t*+ experimental conditions a) 11ms and b) 13ms

By analyzing the data from Figs. 3 and 4, the heating rate tends to increase proportionally as the positive polarities of the welding increase. The welding condition *t*+ = 13ms reach the highest temperature; therefore it has the highest heating rate. In order to determine the effects presented by the thermal analyses, the grain size of the HAZ was measured. Table 2 presents the average size for each experimental welding condition. A correlation between the grain size and the evolution of the positive polarities on the plate must be pointed out. As a matter of fact, the grain size tends to decrease linearly as the adjusted welding condition increases. This fact could be explained by the thermal characteristic of the process. The adjusted condition *t*+ = 13ms has the highest estimated power; consequently, it also induces the highest temperature on the plate. As shown in Fig. 4, consequently, this condition presents the highest heating and cooling rate. Thus, this fast cooling generates a bigger nucleation of the material which leads to a smaller grain size. On the other hand, the adjusted welding condition *t*+ = 2ms has a lower estimated power; consequently it will induce a lower temperature on the plate. As shown in Fig. 3, this condition has the lowest heating and cooling rate of the analyzed cases. Since the cooling rate is lower, a grain growth may be noticed.

Table 2. Average grain size for each welding condition.

Adjusted (*t*+) (ms)	**Adjusted (*t*-) (ms)**	**Estimated power (W)**	**Grain size (µm)**
2	20	2037	80.01
7	20	2187	57.39
11	20	2335	46.96
13	20	2702	40.00

A linear dependence of the grain size in relation to the temperature may be noticed. Figure 5 presents a linear fit approximation for the data presented in Table 2.

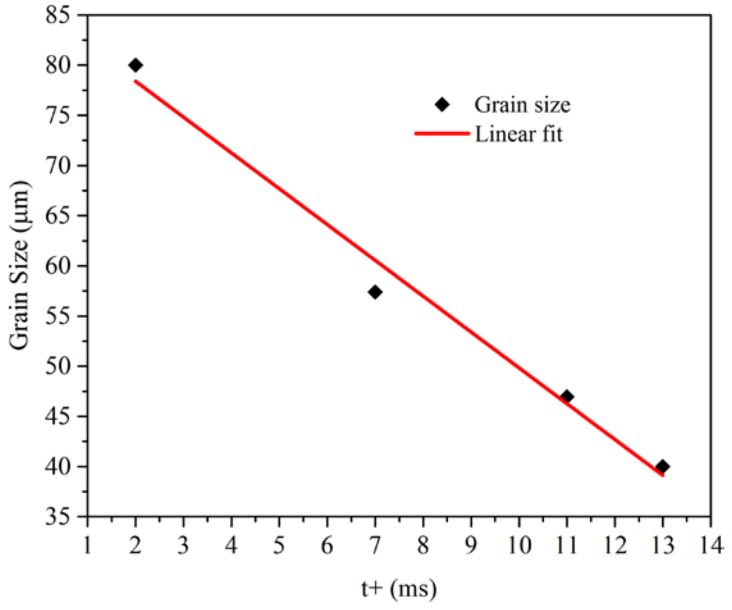

Figure 5. Grain size versus positive polarity condition.

The cooling rate was also studied after the welding torch was turned off. In this analysis, the *P* points have not displayed a significant difference when compared to the same welding condition i.e. all *P* points presented almost the same cooling rate. Consequently, the microstructural change for this welding experiment occurred when the GTA torch was on. The cooling rate also presented a similar profile for the different *t+* welding conditions. Figure 6 presents the cooling rate, aforementioned as the negative heating rate, for the *P* points in relation to the time.

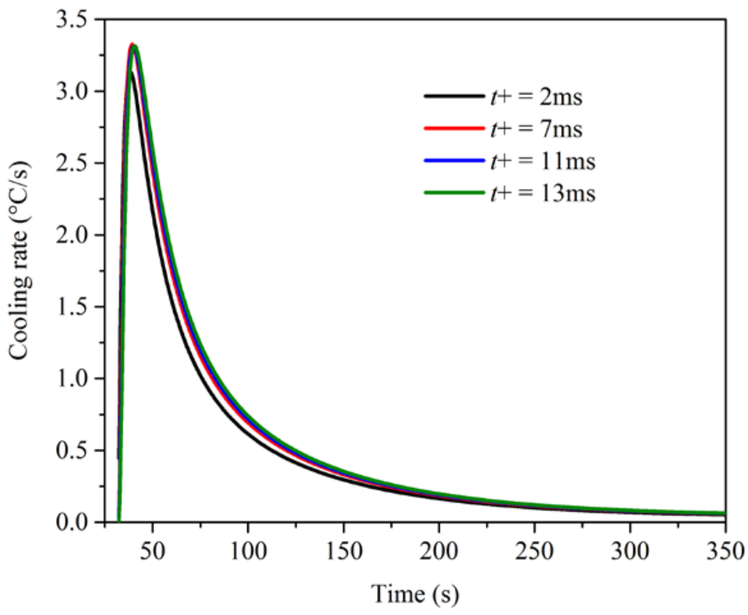

Figure 6: Numerical cooling rate for all *P* points after the welding torch is turned off.

Figure 7 presents the micrographs obtained for the four experimental conditions. The polarities *t+* = 11ms and *t+* = 13ms presented a eutectic phase. In all cases, dendritic structures were found in the fusion zone.

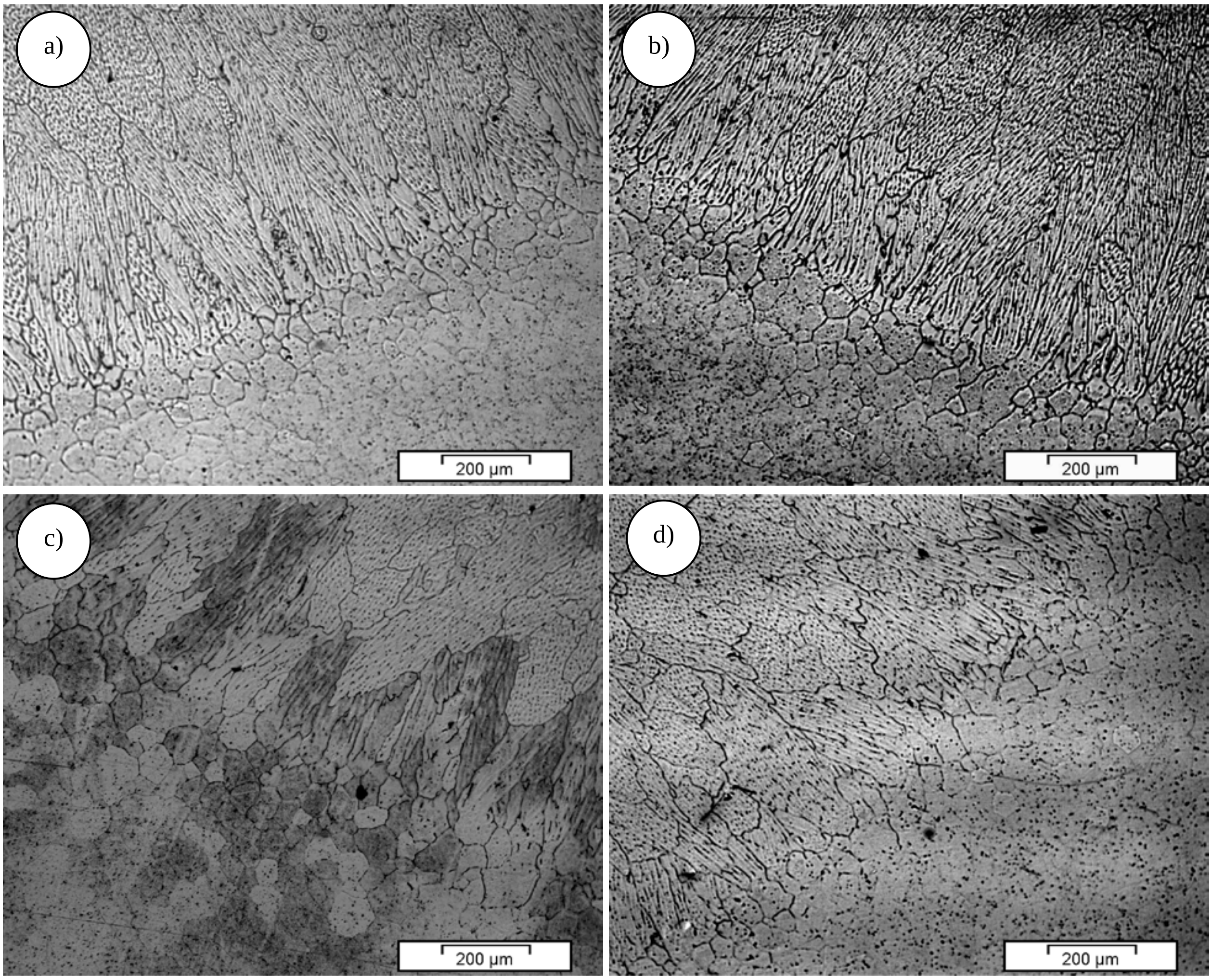

Figure 7: Microstructural analysis for the *t*+ welding conditions a) 2ms; b) 7ms; c) 11ms and d) 13ms

4. CONCLUSIONS

This paper presented a thermal analysis of the HAZ on numerical heat transfer model based software. A linear dependence of the grain size in relation to the positive polarity was noticed. The cooling rate of the six analyzed temperature points increase as the points are close to the surface of the sample and the positive polarity intensifies. The microstructural changes also occurred when the welding torch was. The heat transfer loss (cooling rate) after the GTA torch was turned off is the same for the points on the fusion zone, HAZ and base material. The software proved to be a good and cheap way to analyze the welding in the HAZ. The software could also be adapted to other welding processes. Therefore, it could improve welding processes in general.

5. ACKNOWLEDGEMENTS

The authors would like to thank CNPq, CAPES and FAPEMIG for their financial support.

6. REFERENCES

Ahmad, M., Akhter, J. I., Akhtar, M., Iqbal, M., 2007. “Microstructure and characterization of phases in TIG welded joints of Zircaloy-4 and stainless steel 304-L”. *Journal of Materials Science*, Vol. 42 (1), pp.328-331.

Amirthalingam, M., Hermans, M., Richardson, I., 2009. “Microstructural Development during Welding of Silicon and Aluminum-Based Transformation-Induced Plasticity Steels – Inclusion and Elemental Partitioning Analysis”. *Metallurgical and Materials Transactions A*, Vol. 40 (4), pp.901-909.

Carvalho, S. R., Lima e Silva, S. M. M., Guimaraes, G., 2006. “Thermal Analysis Using Inverse Technique Applied to an Aluminum Alloy GTAW”, *International Heat Transfer Conference*, Vol. 13, 12p.

Casalino, G. and Panella, F.W., 2007. “Microstructural analysis of AISI 304 bars welded with high speed pulsed discharges”. *Journal of Materials Processing Technology*, Vol. 191, pp. 149-152.

Chen, W.L. and Yang., Y.C., 2010. “Inverse Problem of Estimating in the Heat Flux at the Roller / Workipiece Interface During a Rolling Process”. *Applied Thermal Engineering*, Vol. 30, pp. 1274-1254.

Dagner, J., Friedrich, J., Müller, G., 2008. “Numerical Study on the Prediction of Microstructure Parameters by Multi-Scale Modeling of Directional Solidification of Binary Aluminum – Silicon Alloys”. *Computational Materials Science*, Vol. 43 (4), pp. 872-885.

Ghosh, M., Kumar, K., Mishra, R.S., 2010. “Analysis of microstructural evolution during friction stir welding of ultrahigh-strength steel”, *Scripta Materialia*, Vol. 63 (8), pp. 851-854.

Grill, A., 1981. “Effect of Arc Oscillations on the Temperature Distribution and Microstructure in GTA Tantalum Welds”. *Metallurgical and Materials Transactions B*, Vol. 12 (4), pp. 667-674.

Goldak, J.A. and Akhlaghi, M., 2005. *Computation Welding Mechanics*. Springer.

Gonçalves, C.V., Carvalho, S.R., Guimaraes, G., 2010. “Application of optimization techniques and the enthalpy method to solve a 3D-inverse problem during a TIG welding process”, Materials and Design Vol 30, pp 2398-2402.

Gostimirovic, M., Kovac, P., Sekulic, M., 2011. “An Inverse Heat Transfer Problem For Optimization of the Thermal Processing in Maching”. *Sadhana*, Vol. 36 (4), pp. 489-504.

Hajbagheri, F. A., Bozorg, S. F. Kashani. 2008. “Microstructure and wear assessment of TIG surface alloying of CP-titanium with silicon”, *Journal of Materials Science*, Vol. 43(17), pp. 5720-5727.

Karkhin, V.A., Pittner, A., Schwenk, C., Rethmeier, M., 2011. “Simulation of Inverse Heat Condution Problems in Fusion Welding With Extended Analytical Heat Source Models”. *Frontiers of Materials Science*, Vol. 5 (2), pp. 119-125.

Kumar, T.S., Balasubramanian, V., Babu, S., Sanavullah, M.Y., 2007. “Effect of Pulsed Current GTA Welding Parameters on the Fusion Zone Microstructure of AA6061 Aluminum Alloy”. Metals and Materials International, Vol. 13 (4), pp. 345-351.

Magalhães, E.S., Carvalho, S.R., Lima e Silva, A.L.F., Lima e Silva, S.M.M., 2015. “The use of non-linear inverse problem and enthalpy method in GTAW process of aluminum”. *International Communications in Heat and Mass Transfer*, Vol. 66, pp. 114-121.

Manti, R., Dwivedi, D.K., Argarwal, A., 2008. “Microstructure and hardness of Al-Mg-Si weldments produced by pulse GTA welding”, *The International Journal of Advanced Manufacturing Technology*, Vol. 36 (3-4), pp. 263-269.

Mohammadtaheri, M., 2012. “A New Metallographic Technique for Revealing Grain Boundaries in Aluminum Alloys”. *Metallography, Microstructure, and Analysis*, Vol. 1, pp. 224-226.

Norman, A.F., Drazhener, V., Prangnell P.B., 1999. “Effect of welding parameters on the solidification microstructure of autogenous TIG welds in an Al-Cu-Mg-MN alloy”. *Materials Science and Engineering A*, V. 259(1), pp. 53-64.

Unfried, J.S., Garzón, C.M., Giraldo, J.E., 2009 “Numerical and Experimental Analysis of Microstructure evolution during arc welding in armor plate steels”. *Journal of Materials Processing Technology*, Vol. 209 (4), pp. 1688-1700.

Vanderplaats, G. N., 2005. *Numerical optimization techniques for engineering design*. McGraw Hill USA, 4th edition, 465 p.

Vishwakarma, K.R., Richards, N.L., Chaturvedi, M.C., 2008. “Microstructural analysis of fusion and heat affected zones in electron beam welded ALLVAC® 718PLUS^{TM} superalloy”. *Materials Science and Engineering A*, Vol. 480, pp. 517-528.

Yu-Ching, Y., Wen-Lin, C., Haw-Long, L., 2011. “A Nonlinear Inverse Problem in Estimating the Heat Generation in Rotary Friction Welding”, *Numerical Heat transfer A*, Vol. 59, pp. 130-149.

7. RESPONSIBILITY NOTICE

The authors are the only responsible for the printed material included in this paper.